Dispersion of the dielectric function of a charge-transfer insulator

R. O. Kuzian
Institute for Problems of Materials Sciences, Krzhizhanovskogo 3, 03180 Kiev, Ukraine

R. Hayn
Leibniz-Institut für Festkörper- und Werkstoffforschung Dresden, P.O. Box 270016, D-01171 Dresden, Germany and Laboratoire Matériaux et Microélectronique de Provence, 49 Rue Joliot-Curie, IRPHE, F-13384 Marseille Cedex 13, France

A. F. Barabanov
Institute for High Pressure Physics, 142190 Troitsk, Moscow Region, Russia
(Received 2 April 2003; published 7 November 2003)

We study the problem of dielectric response in the strong-coupling regime of a charge-transfer insulator. The frequency and wave-number dependence of the dielectric function $\varepsilon(\mathbf{q},\omega)$ and its inverse $\varepsilon^{-1}(\mathbf{q},\omega)$ is the main object of consideration. We show that the problem, in general, cannot be reduced to a calculation within the Hubbard model, which takes into account only a restricted number of electronic states near the Fermi energy. The contribution of the rest of the system to the longitudinal response [i.e., to $\varepsilon^{-1}(\mathbf{q},\omega)$] is essential for the whole frequency range. With the use of the spectral representation of the two-particle Green's function we show that the problem may be divided into two parts: into the contributions of the weakly correlated subsystem and the Hubbard subsystem. For the latter we propose an approach that starts from the correlated paramagnetic ground state with strong antiferromagnetic fluctuations. We obtain a set of coupled equations of motion for the two-particle Green's function that may be solved by means of the projection technique. The solution is expressed by a two-particle basis that includes the excitonic states with electron and hole separated at various distances. We apply our method to the multiband Hubbard (Emery) model that describes layered cuprates. We show that strongly dispersive branches exist in the excitonic spectrum of the ''minimal'' Emery model $(1/U_d = U_p = t_{pp} = 0)$ and consider the dependence of the spectrum on finite oxygen hopping t_{pp} and on-site repulsion U_p. The relationship of our calculations to electron-energy-loss spectroscopy is discussed.

DOI: 10.1103/PhysRevB.68.195106 PACS number(s): 71.35.−y, 71.27.+a, 79.20.Uv, 74.72.−h

I. INTRODUCTION

The importance of many-body effects for the description of dielectric response of insulating solids is generally accepted. In the neighborhood of the fundamental absorption threshold bound exciton lines and continuum excitons drastically change the spectrum. Recently, it has been realized that the excitons in charge-transfer insulators (CTI) possess unusual features connected with the strongly correlated character of the antiferromagnetic (AFM) ground state in these compounds. The most pronounced peculiarity consists in the existence of exciton branches with substantially larger dispersion compared with the one-particle excitations.[1,2] This behavior has a formal analogy with that of the Frenkel exciton[3] that acquires a finite effective mass although both, electron and hole, have infinite masses,[4] but in CTI it has a completely different origin.

The experimental technique suitable for the observation of the exciton dispersion is the electron-energy-loss spectroscopy (EELS).[5] What is actually measured in transmission EELS experiments is the partial cross section[6,7] that may be decomposed into an amplitude factor and a dynamic structure factor

$$\frac{d^2\sigma}{d\Omega\, dE} = \frac{4}{(a_0)^2 q^4} S(\mathbf{q},\omega).$$

The dynamic structure factor characterizes the linear response of the whole electronic system on *longitudinal* electric fields with the momentum $\mathbf{q}$ and frequency ω (the ionic contribution may be neglected for the considered frequency range of the order of several eV). Pronounced peaks in $S(\mathbf{q},\omega)$ are called excitons.[8] They may correspond to discrete lines in the excitation spectrum of the solid or to resonances in the continuum part of the spectrum.

For the theoretical description of excitonic features in conventional semiconductors and insulators the following scheme is used (the key references are Refs. 4,9–12). First, the quasiparticle excitation spectrum is found empirically[4,9,12] or from first principles.[10,11] It is essential that the spectrum of the N-electron system consists mainly of a continuum of electron-hole pairs whose electron or hole quasiparticle excitations are close to eigenstates of the $(N+1)$- or $(N-1)$-electron system, respectively, with definite quasimomenta *and* energy.[13] The quasiparticle spectrum is usually obtained from the self-consistent-field (SCF) approach. Next, the electron-hole interaction is taken into account. Then the problem for two quasiparticles interacting via the medium is solved. It is crucial that the ground state may be viewed as an occupied valence band that is separated from the first excited state by an energy gap.

For the CTI the above scheme should be revised beginning from the first step. The CTI has an odd number of electrons per formula unit. That is why the SCF calculations usually give a *metallic* ground state for the CTI and a gapless

excitation spectrum. More elaborate SCF methods such as the unrestricted Hartree-Fock method or its modern version LDA+U predict an AFM long-range order in the ground state and a gap in the excitation spectrum. Nevertheless, the nature of excitations and the ground-state fluctuations are not caught by these approaches. Let us recall that any CTI remains insulating and shows excitonic features in optics and EELS spectra above the Néel temperature, i.e., in the *paramagnetic* state (with short-range AFM correlations). For strongly correlated systems the electron-electron interaction should be taken into account beyond the mean-field level. This is possible within the framework of Hubbard-like models in the restricted subspace of orbitals close to the Fermi level.

The description of exciton physics in CTI is possible within the framework of one-band models,[14–17] but more detailed and realistic information may only be obtained from the multiband Hubbard (Emery) model that explicitly includes ligand ion degrees of freedom. For quasi-one-dimensional cuprates the Emery model was considered in Refs. 18–21. The phenomenon of spin-charge separation that is characteristic to one dimension introduces a specific physics into the exciton formation. The mobility of a single electron or hole in 1D is not suppressed by spin correlations and the exciton dispersion is comparable with the one-particle dispersion.

In quasi-two-dimensional cuprates the situation is different. Due to AFM correlations the bandwidth of the one-particle motion is of the order of the AFM exchange integral J which is considerably smaller than the bare hopping t, and the exciton dispersion is of the order of t. The authors of Ref. 22 proposed a qualitative physical explanation of the large exciton dispersion in layered cuprates: the propagation of an electron-hole pair does not disturb the AFM background, in contrast to the motion of a single electron or hole. Unfortunately, the calculations of Ref. 22 do *not* support this idea since they give no dispersion in the absence of oxygen on-site Coulomb repulsion U_p and direct O-O hopping t_{pp}, which was also pointed out in Ref. 18. One should expect a qualitative description of the EELS spectra[1,2] already within the ''minimal'' version of the Emery model ($1/U_d = U_p = t_{pp} = 0$), which can be refined by taking into account additional parameters, e.g., t_{pp} or U_p. On the contrary, the authors of Ref. 22 had to assume quite unrealistic parameter values to fit the experimental spectra.

In this paper we outline an approach to calculate the longitudinal and the transverse dielectric responses (Sec. II) for CTI within the framework of the multiband Hubbard model (Sec. III). Introducing an analogy to Wannier's excitonic representation[23] we obtain a set of coupled equations of motion for the two-particle Green's function that may be solved by means of the projection technique[24] (Sec. IV). It is substantial that the method allows a systematic improvement of approximations. In order to retain only the essential properties of CTI we first consider the minimal version of the Emery model describing the CuO_2 plane of high-T_c superconductors and their parent compounds. The model reflects the main features of CTI: the existence of two kinds of states—strongly correlated ''copper'' states with the prohibition of double occupancy and uncorrelated ''oxygen'' states; the undoped plane has one hole per unit cell, and is a quantum two-dimensional AFM insulator possessing no long-range order at any finite temperature; the charge excitation corresponds to the transfer of a hole from copper to the adjacent oxygen site. In Sec. V, we discuss the solution of our equations within the small exciton basis and its dependence on various parameters of the extended Emery model. We obtain an appreciable exciton dispersion and a rough, qualitative agreement with the experimental spectra already within the minimal version of the Emery model.

II. DENSITY-DENSITY CORRELATION FUNCTION

The dynamic structure factor is related to the density-density correlation function

$$S(\mathbf{q},\omega) \equiv \frac{1}{2\pi N}\int_{-\infty}^{\infty} dt e^{-\imath\omega t}\langle \hat{n}_{\mathbf{q}}(t)\hat{n}_{-\mathbf{q}}(0)\rangle = \frac{1}{\pi}\frac{1}{\exp(-\beta\omega)-1}\mathrm{Im}N_{\mathbf{q}}(\omega), \tag{1}$$

where

$$\hat{n}_{\mathbf{q}} = \frac{1}{\sqrt{N}}\sum_{\mathbf{r},s}\exp(-\imath\mathbf{q}\cdot\mathbf{r})(a^{\dagger}_{\mathbf{r},s}a_{\mathbf{r},s} - \langle a^{\dagger}_{\mathbf{r},s}a_{\mathbf{r},s}\rangle) \tag{2}$$

is the electronic density operator in the localized basis, the summation runs over all lattice sites $\mathbf{r}$ and orbital sorts s; $\langle\cdots\rangle$ means the thermodynamic average. For $\beta\omega \gg 1$ we have

$$S(\mathbf{q},\omega) \approx -\frac{1}{\pi}\mathrm{Im}N(\mathbf{q},\omega),$$

where

$$N(\mathbf{q},\omega) \equiv \langle\langle \hat{n}_{\mathbf{q}} | \hat{n}_{-\mathbf{q}}\rangle\rangle = -i\int_0^{\infty} dt e^{-\imath\omega t}\langle[\hat{n}_{\mathbf{q}}(t),\hat{n}_{-\mathbf{q}}(0)]\rangle \tag{3}$$

is the retarded Green's function that defines the inverse dielectric function

$$\varepsilon^{-1}(\mathbf{q},\omega) = 1 + \frac{4\pi e^2}{v_c q^2}N(\mathbf{q},\omega), \tag{4}$$

with v_c being the volume of the unit cell and e the electronic charge. We neglect here the local field effects (coupling with the Fourier components with $\mathbf{q}' = \mathbf{q} + \mathbf{G}$, $\mathbf{G}$ being a reciprocal lattice vector). The function $N(\mathbf{q},\omega)$ describes the response to the *unscreened* external potential. It requests the account of the macroscopic electric field, i.e., the long-range part of the Coulomb interaction. The latter is responsible for the splitting into longitudinal and transverse excitons for small wave number which is analogous to the splitting into longitudinal and transverse optical phonons.[9] The response to the total, *screened* potential is given by[25]

$$N_s(\mathbf{q},\omega) = \varepsilon(\mathbf{q},\omega)N(\mathbf{q},\omega), \tag{5}$$

then

$$\varepsilon(\mathbf{q},\omega)=1-\frac{4\pi e^2}{v_c q^2}N_s(\mathbf{q},\omega). \tag{6}$$

In the diagrammatic language the linear response to the total field may be expressed by the polarization operator where only irreducible graphs (which do not contain the contribution of the macroscopic electric field) should be taken into account.[26,27] The random-phase approximation results in

$$N(\mathbf{q},\omega)=\frac{N_s(\mathbf{q},\omega)}{1-\frac{4\pi e^2}{v_c q^2}N_s(\mathbf{q},\omega)}, \tag{7}$$

which follows from Eqs. (5) and (4) and is *exact* for $q\to 0$, as it was shown in Ref. 26.

The construction of Hubbard-like models for strongly correlated systems has an input from LDA band-structure calculations where the screening of the long-range part of the Coulomb interaction is already taken into account. The Hubbard terms arise from the short-range residual interaction. Thus, the density response function $N_H(\mathbf{q},\omega)$ calculated within the Hubbard model is an approximation to $N_s(\mathbf{q},\omega)$.[14] In other words, it describes the motion of transverse (or ''mechanical'' by Agranovich's[28] terminology) excitons.

Using the spectral representation we may write

$$N_s(\mathbf{q},z)=\int_0^\infty\left[-\frac{1}{\pi}\mathrm{Im}N_s(\mathbf{q},\omega')\right]\frac{2\omega' d\omega'}{z^2-\omega'^2}=\int_0^{\omega_0}+\int_{\omega_0}^\infty$$

$$=N_H(\mathbf{q},z)+N_\infty(\mathbf{q},z). \tag{8}$$

Here we bear in mind that the Hubbard model contributes to transitions in the low-frequency region $\omega<\omega_0$ with ω_0 of the order of the bandwidth, and the electrons of the rest of the solid are excited only at higher energies. In zero approximation we may assume that in the frequency region $\omega>\omega_0$, the electronic polarization of the rest of the solid follows immediately the external field

$$N_\infty(\mathbf{q},z)\approx N_\infty(\mathbf{q},0).$$

In other words, the Hubbard model is embedded into the medium with dielectric permeability

$$\varepsilon_\infty(\mathbf{q})=1-\frac{4\pi e^2}{v_c q^2}N_\infty(\mathbf{q},0).$$

In fact, ε_∞ may have its own dispersion and may be quite anisotropic for layered or quasi-one-dimensional compounds. In principle, it should be taken from, e.g., LDA calculations (we have assumed that the rest of solid is uncorrelated) or from experiment. It is obvious that the peak positions of the loss function

$$L(\mathbf{q},\omega)\equiv-\mathrm{Im}[\varepsilon^{-1}(\mathbf{q},\omega)] \tag{9}$$

and their intensity strongly depend on the value of $\varepsilon_\infty(\mathbf{q})$. Usually, one neglects the $\mathbf{q}$-dependence and the anisotropy of ε_∞, but it is a crude approximation, as well as another one which assumes $\varepsilon(\mathbf{q},0)=\mathrm{const}$ (see the discussion in Sec. V). For a quantitative description of EELS experiments the detailed knowledge of $\varepsilon_\infty(\mathbf{q})$ is necessary. Then the total dielectric function is

$$\varepsilon(\mathbf{q},\omega)=\varepsilon_\infty-\frac{4\pi e^2}{v_c q^2}N_H(\mathbf{q},\omega)\equiv\varepsilon_\infty\varepsilon_H \tag{10}$$

and its inverse is

$$\varepsilon^{-1}(\mathbf{q},\omega)=\varepsilon_\infty^{-1}\varepsilon_H^{-1}.$$

For the dielectric function of the Hubbard model ε_H, the usual sum rule holds

$$\int_0^\infty\omega\mathrm{Im}\varepsilon_H(\mathbf{q},\omega)d\omega=-\int_0^\infty\omega\mathrm{Im}\varepsilon_H^{-1}(\mathbf{q},\omega)d\omega$$

$$=\frac{\pi}{2}\frac{4\pi e^2}{\varepsilon_\infty v_c q^2}\langle[[\hat{n}_\mathbf{q},\hat{H}_H],\hat{n}_{-\mathbf{q}}]\rangle,$$

where $\hat{H}_H$ is the Hubbard model Hamiltonian and the operator $\hat{n}_\mathbf{q}$ acts in the subspace of orbitals which enter into $\hat{H}_H$ [i.e., the summation over s in Eq. (2) is restricted to these orbitals]. Then for the total dielectric function approximated by Eq. (10) we have

$$-\int_0^\infty\omega\mathrm{Im}\varepsilon^{-1}(\mathbf{q},\omega)d\omega=\frac{\pi}{2}\frac{4\pi e^2}{\varepsilon_\infty^2 v_c q^2}\langle[[\hat{n}_\mathbf{q},\hat{H}_H],\hat{n}_{-\mathbf{q}}]\rangle$$

$$=\frac{1}{\varepsilon_\infty^2}\int_0^\infty\omega\mathrm{Im}\varepsilon(\mathbf{q},\omega)d\omega. \tag{11}$$

The factor $1/\varepsilon_\infty^2$ arises due to the negligence of the frequency dependence of ε_∞.

III. MODEL HAMILTONIAN AND DENSITY OPERATOR

As we have mentioned in the Introduction, we consider the minimal Emery model that exhibits the essential properties of layered cuprates ($1/U_d=U_p=t_{pp}=0$). Then the total Hamiltonian in hole notation reads

$$\hat{H}_H=\hat{H}_0+\hat{V}, \tag{12}$$

where

$$\hat{H}_0=\Delta\sum_{\mathbf{r},\gamma}\overline{p}^\dagger_{\mathbf{r},\gamma}\overline{p}_{\mathbf{r},\gamma},\quad \hat{V}=t\sum_{\mathbf{R},\alpha,\gamma}(\overline{p}^\dagger_{\mathbf{R}+\mathbf{a}_\alpha,\gamma}\overline{Z}^{0\gamma}_\mathbf{R}+\overline{Z}^{\gamma 0}_\mathbf{R}\overline{p}_{\mathbf{R}+\mathbf{a}_\alpha,\gamma}),$$

and where the Fermi operator $\overline{p}_{\mathbf{r},\gamma}$ annihilates a hole at site $\mathbf{r}$ of the oxygen sublattice with spin projection index γ, the Hubbard projection operator $\overline{Z}^{0\gamma}_\mathbf{R}=\overline{d}_{\mathbf{R}\gamma}(1-n_{\mathbf{R}\bar{\gamma}})$ annihilates a hole with spin index γ on a *singly occupied* copper site, where $\overline{d}_{\mathbf{R}\gamma}$ is the corresponding Fermi operator. The double occupancy of copper sites is thus excluded from Eq. (12). $\hat{H}_0$ includes the on-site energies ($\Delta=\epsilon_p-\epsilon_d$, ϵ_d is taken as zero of energy), $\hat{V}$ is the *p-d* hybridization, $\alpha=x,-x,y,-y$ char-

acterizes the direction of a nearest-neighbor vector **a**; the phase factors in $\hat{V}$ are absorbed into the definition of the operators $\overline{p}_{\mathbf{r},\sigma}, \overline{Z}^{0\gamma}_{\mathbf{R}}$, they do not change the exciton dispersion.

Taking the limit $U_d/\Delta \to \infty$ considerably simplifies the consideration and is a good approximation for weakly doped compounds in a wide range of values $U_d/\Delta > 2$ (see, e.g., Ref. 29). The conditions $U_p = t_{pp} = 0$ are introduced for simplicity and may be easily relaxed (see the Appendix), then the Hubbard on-site term for *p*-orbitals and the direct O-O hopping of the form $\hat{t}_{pp} = -t_{pp}\Sigma_{\langle i,j\rangle,\gamma}\overline{p}^{\dagger}_{\mathbf{r}_i,\gamma}\overline{p}_{\mathbf{r}_j,\gamma}$ are added to $\hat{H}_0$.

It is well known that the Hamiltonian (12) has an insulating ground state and is equivalent to the nearest-neighbor AFM Heisenberg model in the low-energy region. It means that charge fluctuations in $\hat{V}$ are strongly suppressed and that holes are localized. This fact becomes more apparent if we make a canonical transformation of operators of the form

$$\hat{A}_{eff} = \exp(-\hat{S})\hat{A}\exp(\hat{S}) = \hat{A} + [\hat{A}, \hat{S}] + \cdots,$$

where

$$\hat{S} = -\frac{t}{\Delta}\sum_{\mathbf{R},\alpha=\pm x,\pm y,\gamma}(p^{\dagger}_{\mathbf{R}+\mathbf{a}_\alpha,\gamma}Z^{0\gamma}_{\mathbf{R}} - Z^{\gamma 0}_{\mathbf{R}}p_{\mathbf{R}+\mathbf{a}_\alpha,\gamma}).$$

Then $\hat{H}_H$ becomes

$$\hat{H}_{eff} \approx \hat{H}_0 - 4\tau\sum_{\mathbf{R},\gamma} Z^{\gamma\gamma}_{\mathbf{R}} + \tau\sum_{\mathbf{R},\alpha 1,\alpha 2,\gamma} p^{\dagger}_{\mathbf{R}+\mathbf{a}_{\alpha 1},\gamma_1}p_{\mathbf{R}+\mathbf{a}_{\alpha 2},\gamma_2}(Z^{00}_{\mathbf{R}}\delta_{\gamma_1\gamma_2} + Z^{\gamma_2,\gamma_1}_{\mathbf{R}}) - \tau\sum_{\mathbf{R},\alpha,\gamma_1} Z^{\gamma_1 0}_{\mathbf{R}+\mathbf{g}_\alpha}Z^{0\gamma_1}_{\mathbf{R}} + \hat{J}_s \quad (13)$$

(see also Ref. 30 for the notation). Here *p* and *Z* mean transformed operators, $\hat{J}_s$ is the AFM copper-copper superexchange interaction, and **g** points to neighboring copper sites. Strictly speaking, Hamiltonian (13) is obtained under the condition $t/\Delta \ll 1$, and its parameters are $\tau = t^2/\Delta$ and the AFM exchange $J \propto t^4/\Delta^3$. Nevertheless, it may be applied in a wider range $t/\Delta < 1$ with renormalized values of τ and *J*.

The advantage of using the effective Hamiltonian (13) instead of the bare one, Eq. (12), consists in excluding irrelevant zero-point charge fluctuations. Then the coupling of carriers with spin fluctuations which governs the low-energy physics of CTI becomes apparent. It is essential that the effective Hamiltonian (13) does not contain transitions between *p*- and *Z*-states, in other words, it never creates a particle-hole state out of the dielectric state. In this sense it resembles the starting Hamiltonian for the transverse exciton motion in conventional insulators. This allows us to introduce an analog of Wannier's excitonic representation for the description of the electron-hole pair dynamics.

The bare density operator

$$\hat{n}_{\mathbf{q}} = \frac{1}{\sqrt{N}}\left[\sum_{\mathbf{R},\sigma}\exp(-\imath\mathbf{q}\cdot\mathbf{R})(\overline{Z}^{\sigma\sigma}_{\mathbf{R}} - \langle\overline{Z}^{\sigma\sigma}_{\mathbf{R}}\rangle) + \sum_{\mathbf{s}}\exp(-\imath\mathbf{q}\cdot\mathbf{s})(\overline{p}^{\dagger}_{\mathbf{s},\sigma}\overline{p}_{\mathbf{s},\sigma} - \langle\overline{p}^{\dagger}_{\mathbf{s},\sigma}\overline{p}_{\mathbf{s},\sigma}\rangle)\right] \quad (14)$$

(**s** runs over O sublattice) is transformed to

$$\hat{n}_{\mathbf{q}} = \frac{1}{\sqrt{N}}\left\{\sum_{\mathbf{R},\sigma}\exp(-\imath\mathbf{q}\cdot\mathbf{R})\left[Z^{\sigma\sigma}_{\mathbf{R}} + \frac{t}{\Delta}\sum_{\alpha=\pm x,\pm y}(p^{\dagger}_{\mathbf{R}+\mathbf{a}_{\alpha'},\sigma}Z^{0\sigma}_{\mathbf{R}} + Z^{\sigma 0}_{\mathbf{R}}p_{\mathbf{R}+\mathbf{a}_{\alpha'},\sigma})\right] + \sum_{\mathbf{R},\alpha=+x,+y}\exp[-\imath\mathbf{q}\cdot(\mathbf{R}+\mathbf{a}_\alpha)] \times\left[p^{\dagger}_{\mathbf{R}+\mathbf{a}_{\alpha'},\sigma}p_{\mathbf{R}+\mathbf{a}_{\alpha'},\sigma} - \frac{t}{\Delta}[(Z^{\sigma 0}_{\mathbf{R}} + Z^{\sigma 0}_{\mathbf{R}+2\mathbf{a}_\alpha})p_{\mathbf{R}+\mathbf{a}_\alpha,\sigma} + \text{H.c.}]\right]\right\}. \quad (15)$$

Note that in the second line of Eq. (15) (in the sum over the oxygen sublattice), $\mathbf{a}_\alpha$ lies only in the same cell as **R**. Collecting the terms surrounding a Cu site, we have

$$\hat{n}_{\mathbf{q}} = \tilde{n}_{\mathbf{q}} + \frac{1}{\sqrt{N}}\frac{t}{\Delta}\sum_{\mathbf{R},\sigma}\exp(-\imath\mathbf{q}\cdot\mathbf{R})\sum_{\alpha=\pm x,\pm y}(p^{\dagger}_{\mathbf{R}+\mathbf{a}_{\alpha'},\sigma}Z^{0\sigma}_{\mathbf{R}} + Z^{\sigma 0}_{\mathbf{R}}p_{\mathbf{R}+a_{\alpha,\sigma}})[1-\exp(-\imath\mathbf{q}\cdot\mathbf{a}_\alpha)]$$
$$= \tilde{n}_{\mathbf{q}} + \frac{1}{\sqrt{N}}\frac{t}{\Delta}\sum_{\mathbf{R}}\exp(-\imath\mathbf{q}\cdot\mathbf{R})\sum_{\alpha\pm x,\pm y}(\psi^{\dagger}_{\mathbf{R},\mathbf{a}_\alpha} + \psi_{\mathbf{R},\mathbf{a}_\alpha}) \times[1-\exp(-\imath\mathbf{q}\cdot\mathbf{a}_\alpha)], \quad (16)$$

where the operator

$$\psi_{\mathbf{R},\alpha} \equiv \sum_{\gamma} Z^{\gamma,0}_{\mathbf{R}}p_{\mathbf{R}+\mathbf{a}_\alpha,\gamma} \quad (17)$$

annihilates an electron-hole pair with minimal distance, and

$$\tilde{n}_{\mathbf{q}} \equiv \frac{1}{\sqrt{N}}\left[\sum_{\mathbf{R},\sigma}\exp(-\imath\mathbf{q}\cdot\mathbf{R})(Z^{\sigma\sigma}_{\mathbf{R}} - \langle\overline{Z}^{\sigma\sigma}_{\mathbf{R}}\rangle) + \sum_{\mathbf{s}}\exp(-\imath\mathbf{q}\cdot\mathbf{s})(p^{\dagger}_{\mathbf{s},\sigma}p_{\mathbf{s},\sigma} - \langle\overline{p}^{\dagger}_{\mathbf{s},\sigma}\overline{p}_{\mathbf{s},\sigma}\rangle)\right]. \quad (18)$$

As we have mentioned above, the effective Hamiltonian (13) conserves the number of particles in every band. Therefore $\tilde{n}_{\mathbf{q}} = 0$ gives no contribution to N_H . Having operator (16) we may proceed with the calculation of the density-density response function (3).

IV. ELECTRON-HOLE PAIR DYNAMICS

The problem of the dielectric function (10) calculation is thus reduced to the calculation of the two-particle Green's function

$$N_H(\mathbf{q},\omega)=\langle\langle\Phi_{\mathbf{q}}+\Phi^{\dagger}_{-\mathbf{q}}|\Phi^{\dagger}_{\mathbf{q}}+\Phi_{-\mathbf{q}}\rangle\rangle_{\omega}$$
$$=\langle\langle\Phi_{\mathbf{q}}|\Phi^{\dagger}_{\mathbf{q}}\rangle\rangle_{\omega}+\langle\langle\Phi_{-\mathbf{q}}|\Phi^{\dagger}_{-\mathbf{q}}\rangle\rangle_{-\omega} \quad (19)$$

where

$$\Phi_{\mathbf{q}}\equiv\frac{t}{\Delta}\sum_{\alpha}(1-\exp(-\imath\mathbf{q}\cdot\mathbf{a}_{\alpha})]\psi_{\mathbf{q},\alpha},$$

$$\psi_{\mathbf{q},\alpha}=\frac{1}{\sqrt{N}}\sum_{\mathbf{R}}\exp(-\imath\mathbf{q}\cdot\mathbf{R})\psi_{\mathbf{R}\alpha}, \quad (20)$$

and where we used again the conservation of particle numbers in the electron and the hole subsystem that excludes anomalous Green's functions such as $\langle\langle\Phi_{\mathbf{q}}|\Phi_{\mathbf{q}}\rangle\rangle_{\omega}$.

The equation of motion

$$\omega\langle\langle\Phi_{\mathbf{q}}|\Phi^{\dagger}_{\mathbf{q}}\rangle\rangle_{\omega}=\langle[\Phi_{\mathbf{q}},\Phi^{\dagger}_{\mathbf{q}}]\rangle+\langle\langle[\Phi_{\mathbf{q}},\hat{H}_{eff}]|\Phi^{\dagger}_{\mathbf{q}}\rangle\rangle_{\omega} \quad (21)$$

generates more complex operators

$$\xi_{\mathbf{R},\alpha,\beta}=\sum_{\gamma_1,\gamma_2}Z^{\gamma_1\gamma_2}_{\mathbf{R}+\mathbf{g}_{\alpha}}Z^{\gamma_2,0}_{\mathbf{R}}p_{\mathbf{R}+\mathbf{g}_{\alpha}+\mathbf{a}_{\beta},\gamma_1}, \quad (22)$$

which annihilate states with an increasing separation between electron and hole, accompanied by spin fluctuations. The set of equations of motion will generate states corresponding to electrons and holes that are more and more separated and dressed by spin fluctuations. These states form a set similar to the excitonic representation for conventional insulators.[4,9,23] The complication that arises in CTI consists in the strong interaction of both electron and hole with AFM fluctuations. The effect of this interaction leads to a strong renormalization of the one-particle bandwidth, but it is partially canceled when electron and hole follow each other.

The set of coupled equations, Eq. (21), may be approximately solved by means of the projection technique. We choose an operator basis $B_{\mathbf{q},i}$ and the definition of the scalar product $\langle[B_{\mathbf{q},i},B^{\dagger}_{\mathbf{q},j}]\rangle$. Within the operator subspace spanned by this basis we are looking for the approximate solution of the eigenvalue problem:

$$[\Psi_{\mathbf{q}},\hat{H}]=E_{\mathbf{q}}\Psi_{\mathbf{q}},\quad \Psi_{\mathbf{q}}=\sum_{i}c_i(\mathbf{q})B_{\mathbf{q},i}. \quad (23)$$

This leads, as usual for a nonorthonormal basis, to the generalized eigenvalue problem

$$\sum_{i}c_i(\mathbf{q})L_{i,j}(\mathbf{q})=E\sum_{i}c_i(\mathbf{q})S_{ij}(\mathbf{q}), \quad (24)$$

where overlap and Liouvillean matrices

$$S_{ij}\equiv\langle[B_i,B^{\dagger}_j]\rangle=\langle B_i,B^{\dagger}_j\rangle,$$

$$L_{ij}\equiv\langle[[B_i,\hat{H}],B^{\dagger}_j]\rangle=\langle[B_i,\hat{H}],B^{\dagger}_j\rangle \quad (25)$$

depend only on spin-spin correlation functions for the system without electron-hole pairs, which is equivalent to the Heisenberg antiferromagnet. The correlation functions may thus be calculated from the Heisenberg model.

System (24) may be solved numerically. Then we find the eigenvectors

$$\Psi^{\lambda}_{\mathbf{q}}=\sum_{i}c^{\lambda}_i(\mathbf{q})B_{\mathbf{q},i}, \quad (26)$$

where λ is the number of the branch in the spectrum. In order to calculate $N_H(\mathbf{q},\omega)$ within our basis, we should expand

$$\Phi_{\mathbf{q}}=\sum_{\lambda}g^{\lambda}(\mathbf{q})\Psi^{\lambda}_{\mathbf{q}}. \quad (27)$$

Then one obtains

$$\langle\langle\Phi_{\mathbf{q}}|\Phi^{\dagger}_{\mathbf{q}}\rangle\rangle_{\omega}=\sum_{\lambda}|g^{\lambda}(\mathbf{q})|^2\langle\langle\Psi^{\lambda}_{\mathbf{q}}|(\Psi^{\lambda}_{\mathbf{q}})^{\dagger}\rangle\rangle_{\omega}$$
$$=\sum_{\lambda}|g^{\lambda}(\mathbf{q})|^2(\omega-E^{\lambda}_{\mathbf{q}})^{-1}, \quad (28)$$

with

$$|g^{\lambda}(\mathbf{q})|^2=\left(\frac{t}{\Delta}\right)^2\left|\sum_{i,\alpha}c^{\lambda}_i(\mathbf{q})S_{i\alpha}[1-\exp(\imath\mathbf{q}\cdot\mathbf{a}_{\alpha})]\right|^2, \quad (29)$$

and finally

$$\varepsilon(\mathbf{q},\omega)=\varepsilon_{\infty}-\frac{4\pi^2e^2}{v_cq^2}\sum_{\lambda}|g^{\lambda}(\mathbf{q})|^2[(\omega-E^{\lambda}_{\mathbf{q}})^{-1}$$
$$-(\omega+E^{\lambda}_{\mathbf{q}})^{-1}]. \quad (30)$$

Let us note that the projection technique allows us to improve the chosen approximation step by step by enlarging the basis set.

V. RESULTS AND DISCUSSION

We have restricted ourself to the minimal basis that describes the electron-hole pair with minimal distance. The basis contains operators (17) and (22) with $\beta=-\alpha$. Then problem (23) has the dimension 8×8. The overlap and Liouvillean matrices are given in the Appendix. Spin-spin correlation functions were taken from the spherically symmetric treatment of an $S=\frac{1}{2}$ Heisenberg AFM model on the square lattice.[31] For a low-temperature $T=0.1J$ and a vanishing frustration parameter $p=0.01$ they have the following values $\langle\hat{\mathbf{S}}_{\mathbf{R}}\cdot\hat{\mathbf{S}}_{\mathbf{R}+\mathbf{g}}\rangle=-0.33$, $\langle\hat{\mathbf{S}}_{\mathbf{R}}\cdot\hat{\mathbf{S}}_{\mathbf{R}+\mathbf{g}_x+\mathbf{g}_y}\rangle=0.20$, $\langle\hat{\mathbf{S}}_{\mathbf{R}}\cdot\hat{\mathbf{S}}_{\mathbf{R}+2\mathbf{g}}\rangle=0.17$. For the on-site energy difference and *p-d* hopping we took the values $\Delta=3.6$ eV and $t=1.3$ eV, which are characteristic to all cuprates.

Figure 1 shows the dispersion of the imaginary part of the dielectric function $\varepsilon_2(\mathbf{q},\omega)\equiv\mathrm{Im}\varepsilon(\mathbf{q},\omega)$. The oxygen on-site repulsion and the O-O hopping were neglected. We see strongly dispersive branches both in the [110] and in the [100] directions.

As we have mentioned above, the comparison with the EELS experiment may have only qualitative character without a detailed knowledge of the background dielectric con-

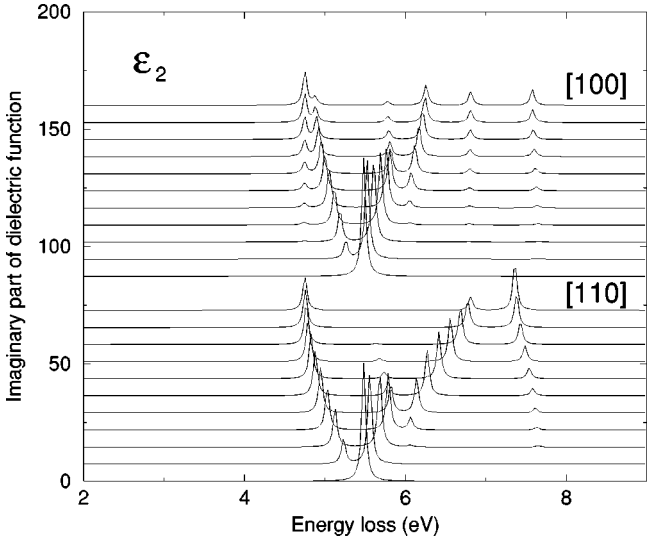

FIG. 1. The imaginary part of dielectric function $\varepsilon_2(\mathbf{q},\omega) \equiv \mathrm{Im}\varepsilon(\mathbf{q},\omega)$ as a function of frequency ω and wave vector $\mathbf{q}$ along two symmetry directions. For each direction the curve number n corresponds to $q_x=\pi n/10a$, a being the lattice constant, $n=0$ for the bottom curve. The parameters are $\Delta=3.6$ eV and $t=1.3$ eV, oxygen on-site repulsion U_p and O-O hopping t_{pp} were neglected.

stant $\varepsilon_\infty(\mathbf{q})$. Figure 2 shows the graphs for the loss function (multiplied by $[\varepsilon_\infty(\mathbf{0})]^2$ in order to have approximately the same normalization as $\varepsilon_2(\mathbf{q},\omega)$ according to Eq. (11)) under the assumption that[22]

$$\varepsilon(\mathbf{q},\omega=0)\approx\varepsilon(\mathbf{q}=\mathbf{0},\omega=0)=4.83. \tag{31}$$

Then the value of ε_∞ was obtained from Eq. (30). In this case the dispersion in the loss function reproduces essentially the dispersion in $\varepsilon(\mathbf{q},\omega)$. The peaks are slightly shifted to higher

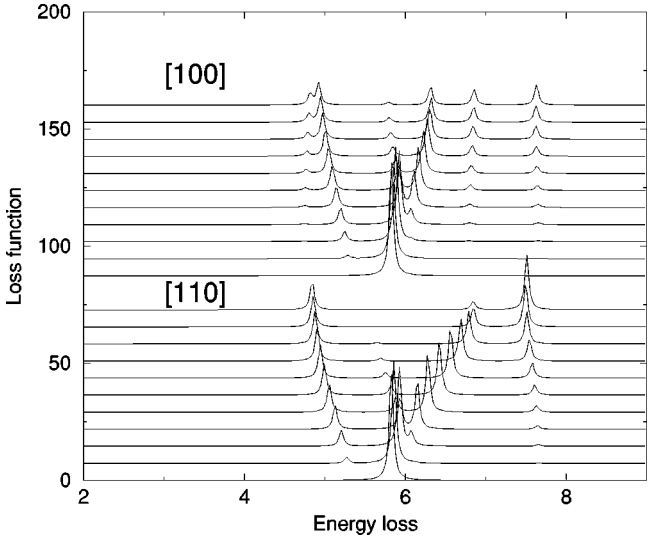

FIG. 2. The loss function $L(\mathbf{q},\omega)\equiv-\mathrm{Im}[\varepsilon^{-1}(\mathbf{q},\omega)]$ (multiplied by $[\varepsilon_\infty(\mathbf{0})]^2$ in order to have aproximately the same normalization as $\varepsilon_2(\mathbf{q},\omega)$) for the same parameters as in Fig. 1 and under the assumption that $\varepsilon(\mathbf{q},\omega=0)\approx\varepsilon(\mathbf{q}=\mathbf{0},\omega=0)=4.83$.

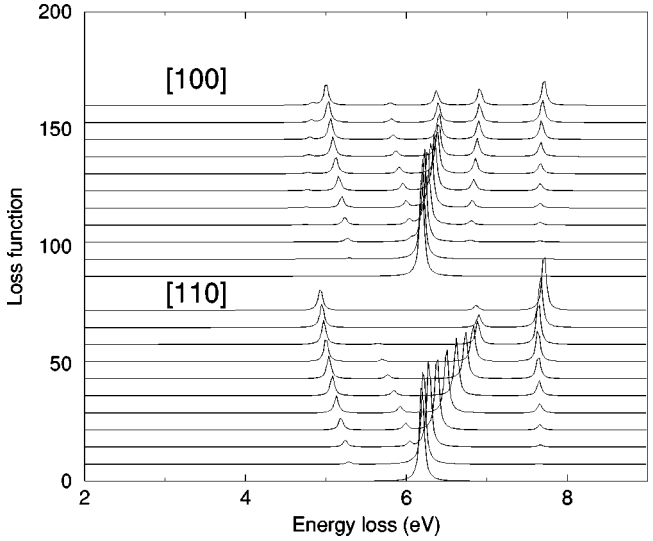

FIG. 3. The loss function for constant $\varepsilon_\infty=2$ for all $\mathbf{q}$ and the parameter set of Fig. 1.

energies. In fact, assumption (31) implies that the dispersion of $N_\infty(\mathbf{q},\omega)$ should follow the dispersion of $N_H(\mathbf{q},\omega)$ in such a way that

$$\varepsilon(\mathbf{q},\omega=0)=1-\frac{4\pi e^2}{v_c q^2}[N_H(\mathbf{q},0)+N_\infty(\mathbf{q},0)]=\text{const},$$

as it follows from Eqs. (8) and (6).

In general, the interplay of $N_H(\mathbf{q},\omega)$ and $N_\infty(\mathbf{q},\omega)$ should be more complex. In order to demonstrate the strong dependence on the value of ε_∞, we plot in Fig. 3 the same graph assuming a constant value $\varepsilon_\infty=2$ for all $\mathbf{q}$'s. We see a qualitative difference with Fig. 2 and may conclude that the dependence of the loss function on ε_∞ is nontrivial. For quasi-one-dimensional compounds a large value of $\varepsilon_\infty\sim 8$ was taken in Refs. 19 and 20. This means that the rest of the solid strongly screens the long-range part of the Coulomb interaction between electrons that enter the Hubbard model. For this situation the poles of $\varepsilon(\mathbf{q},\omega)$ are very close to the poles of $\varepsilon^{-1}(\mathbf{q},\omega)$ and the shape of the loss function is close to the shape of $\varepsilon_2(\mathbf{q},\omega)$. Note also that always $\varepsilon(\mathbf{q},0)>\varepsilon_\infty$ as follows from Eqs. (10) and (30), and with $\varepsilon_\infty=8$ one will receive unrealistically large $\varepsilon(\mathbf{q},0)$.

Let us now show some examples for the dependence of the dielectric function on various parameters of the model. For the reasons outlined above, from now on we consider only figures for $\varepsilon_2(\mathbf{q},\omega)$. As it was mentioned in Sec. III, the model (12) may be generalized in order to include a finite Hubbard repulsion U_p on the oxygen site and a direct oxygen-oxygen hopping t_{pp}.

The dependence on t_{pp} is not very strong for $t_{pp}<\tau$. Let us recall that the addition of the O-O hopping to Hamiltonian (13) within the parameter range $t_{pp}=(0.3\text{–}0.4)\tau$ is essential to describe correctly the angle-resolved photoemission spectroscopy of layered cuprates.[30,32] Figure 4 shows $\varepsilon_2(\mathbf{q},\omega)$ for $t_{pp}=0.4\tau$, and $U_p=0$. We see that the main difference from

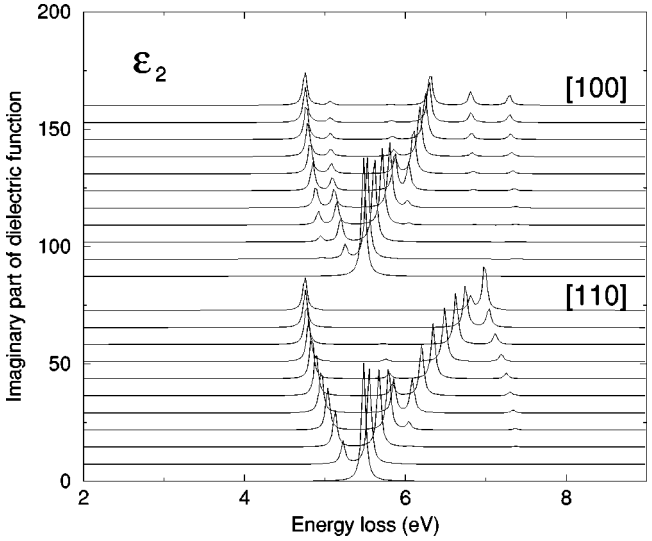

FIG. 4. $\varepsilon_2(\mathbf{q},\omega)$ for $t_{pp}=0.4\tau$ and $U_p=0$. The other parameters are the same as in Fig. 1.

Fig. 1 consists in the redistribution of spectral weight between the different branches of the spectrum.

The spectrum demonstrates a much stronger dependence on U_p. Figure 5 displays $\varepsilon_2(\mathbf{q},\omega)$ for $U_p=4$ eV. We have an almost vanishing dispersion of the lower branches. Let us pay attention to the fact that U_p does not affect the single hole motion. Due to that reason its value is experimentally not well established. Our results show that the dielectric function dispersion is very sensitive to this parameter.

Now let us discuss a very important peculiarity of our figures, namely the absolute position of the intensive peaks in the spectrum of $\varepsilon_2(\mathbf{q},\omega)$. At Γ point $[\mathbf{q}=(0,0)]$ we have one peak with the energy $E_{\mathbf{\Gamma}}=\Delta+4\tau\approx 5.5$ eV. Let us estimate the edge of the electron-hole continuum. It corresponds to the energy that is needed for the excitation of electron and hole which are independent of each other. The operator that annihilates such a state is

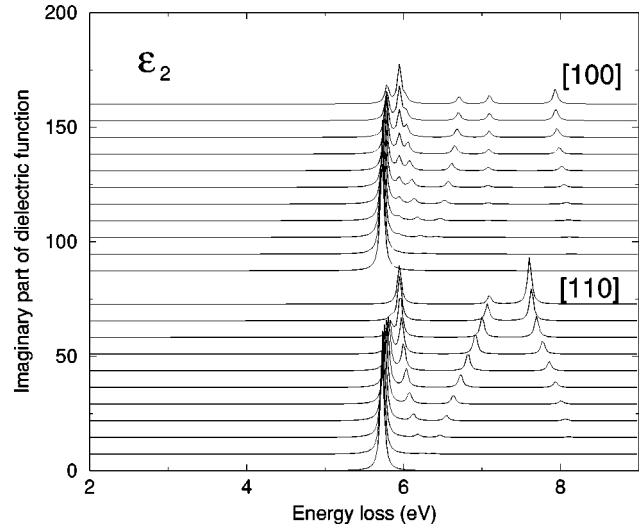

FIG. 5. $\varepsilon_2(\mathbf{q},\omega)$ for $t_{pp}=0$ and $U_p=4$ eV. The other parameters are the same as in Fig. 1.

$$\Psi^{e-h}_{\mathbf{q}}=e_{\mathbf{k}+\mathbf{q}}h_{-\mathbf{k}},\quad [\Psi^{e-h}_{\mathbf{q}},\hat{H}_{eff}]=(\epsilon^{e}_{\mathbf{k}+\mathbf{q}}+\epsilon^{h}_{-\mathbf{k}})\Psi^{e-h}_{\mathbf{q}},$$

where $\epsilon^{e}_{\mathbf{k}}=-(-4\tau-\epsilon^{t-J}_{\mathbf{k}})$ corresponds to the energy of a single-electron quasiparticle, which will be a complex spin-polaron corresponding to the coherent motion in the so-called t-J model, which describes the Z subsystem in Eq. (13) in the absence of holes (with $t^{t-J}=\tau$). $\epsilon^{h}_{\mathbf{k}}=\Delta-\epsilon^{s}_{\mathbf{k}}$ is the energy of the coherent motion of the Zhang-Rice singlet, dressed by spin fluctuations. The minimal energy that one needs to excite such a pair is

$$E^{e-h}_{\min}\approx\Delta-\epsilon^{s}_{\min}-(-4\tau-\epsilon^{t-J}_{\min})\sim\Delta-2.2\tau\approx 2.6\ \text{eV}.$$

Here we have taken into account that the minimum of the spectrum in the t-J model is $\epsilon^{t-J}_{\min}\sim-2\tau$ and that the Zhang-Rice singlet energy is $\epsilon^{s}_{\min}\sim-4.2\tau$.[30] This result indicates that for layered cuprates the excitonic feature is immersed into the electron-hole continuum and represents a resonance rather than a discrete level. Of course, for the final conclusion more detailed calculations should be performed within an enlarged basis set.

Summarizing the calculated spectra we may state a rough, qualitative, agreement with the experimental curves[1,2] already within the minimal version of the Emery model and using a minimal basis set (Figs. 1–3). One may note a remarkable influence of the background dielectric function ε_∞ (Figs. 2 and 3). We found that additional parameters, e.g., t_{pp} or U_p act in different ways. That might improve a future parameter fit of the experimental curves. But the present accuracy is not sufficient for a reliable fit, which has to be reserved for the future.

In this work we have not taken into account the intersite Coulomb repulsion which leads to electron-hole attraction. This term has a twofold influence on the position of the excitonic feature. On one hand, it leads to an effective increase of the fundamental gap and on the other hand it contributes to the electron-hole binding. These tendencies are opposite to each other and should be thoroughly explored in a separate investigation.

ACKNOWLEDGMENTS

This work was supported by DFG (Grant No. 436 UKR 113/49/41) and by RFFR (Project No. 01-12-16719). R.O.K. and A.F.B. acknowledge hospitality at the IFW Dresden, where the main part of this work has been carried out. We wish to thank S.-L. Drechsler and J. Málek for numerous and useful discussions.

APPENDIX

Here we give the formulas for matrices (25) for the Hamiltonian (12) that also includes a finite oxygen on-site repulsion U_p and a direct O-O hopping t_{pp}. The effective Hamiltonian may be generally derived by the following procedure. Let be

$$\hat{H}=\hat{H}_0+\hat{V},\ \ \hat{H}_0=\sum_m |m\rangle E_m\langle m|,\ \ \hat{V}=\sum_m |n\rangle t_{nm}\langle m|, \tag{A1}$$

then the canonical transformation with the operator

$$\hat{S}=\sum_m |n\rangle \frac{t_{nm}}{E_m-E_n}\langle m| \tag{A2}$$

gives $[\hat{H}_0,\hat{S}]=-\hat{V}$, and finally up to the second order

$$\hat{H}_{eff}=\exp(-\hat{S})\hat{H}\exp(\hat{S})=H_0+\frac{1}{2}[\hat{V},\hat{S}]$$

$$=\frac{1}{2}\sum_m |n\rangle\left(\frac{t_{nj}t_{jm}}{E_m-E_j}+\frac{t_{nj}t_{jm}}{E_n-E_j}\right)\langle m|. \tag{A3}$$

Within the operator basis containing Eqs. (17) and (22) we have the following equations of motion for the Hamiltonian containing finite U_p, t_{pp}:

$$[\psi_{\mathbf{R},\alpha},\hat{H}]=E_0\psi_{\mathbf{R},\alpha}+\tau\sum_\beta \psi_{\mathbf{R},\beta}+\tau_u\xi_{\mathbf{R},\alpha,-\alpha}$$
$$+[\tau_u\xi_{\mathbf{R}+\mathbf{g}_\alpha,-\alpha,\alpha}-(\tau_u-\tau)\psi_{\mathbf{R}+\mathbf{g}_\alpha,-\alpha}]$$
$$-t_{pp}\sum_{\beta\neq\alpha,-\alpha}\psi_{\mathbf{R},\beta},$$

$$[\xi_{\mathbf{R},\alpha,-\alpha},\hat{H}]=E_0\xi_{\mathbf{R},\alpha,-\alpha}+\tau\xi_{\mathbf{R}\alpha,-\alpha}$$
$$+\tau\sum_{\beta\neq\alpha} Z^{\gamma_1,\gamma_2}_{\mathbf{R}+\mathbf{g}_\alpha}Z^{\gamma_2,0}_{\mathbf{R}}p_{\mathbf{R}+\mathbf{a}_\beta,\gamma_1}$$
$$-t_{pp}\sum_{\beta\neq\alpha,-\alpha} Z^{\gamma_1,\gamma_2}_{\mathbf{R}+\mathbf{g}_\alpha}Z^{\gamma_2,0}_{\mathbf{R}}p_{\mathbf{R}+\mathbf{a}_\beta,\gamma_1}$$
$$+\tau_u\psi_{\mathbf{R},\alpha}+\tau_u\psi_{\mathbf{R}+\mathbf{g}_\alpha,-\alpha}$$
$$-(\tau_u-\tau)\xi_{\mathbf{R}+\mathbf{g}_\alpha,-\alpha,\alpha}.$$

Here $\tau_u\equiv t^2/(\Delta+U_p)$ and $E_0=\Delta+4\tau+2(\tau-\tau_u)$. It is convenient to introduce the notation

$$\omega_{\mathbf{r}}\equiv\sum_{\gamma,\gamma_1,\gamma_2,\cdots}\langle Z_0^{\gamma,\gamma_1}Z_{\mathbf{g}}^{\gamma_1,\gamma_2}\cdots Z_{\mathbf{r}}^{\gamma_r,\gamma}\rangle.$$

For $\mathbf{r}$ up to the third neighbors $\omega_{\mathbf{r}}$ is expressed via two point correlation functions

$$\omega_g=\frac{1}{2}+\langle\hat{\mathbf{S}}_{\mathbf{R}}\cdot\hat{\mathbf{S}}_{\mathbf{R}+\mathbf{g}}\rangle,$$

$$\omega_{\mathbf{g}_\alpha+\mathbf{g}_\beta}=\frac{1}{4}+2\langle\hat{\mathbf{S}}_{\mathbf{R}}\cdot\hat{\mathbf{S}}_{\mathbf{R}+\mathbf{g}}\rangle+\langle\hat{\mathbf{S}}_{\mathbf{R}}\cdot\hat{\mathbf{S}}_{\mathbf{R}+\mathbf{g}_\alpha+\mathbf{g}_\beta}\rangle. \tag{A4}$$

The Liouvillean and overlap matrices in $\mathbf{k}$-space are then

$$\langle\{\xi_{\mathbf{k}\alpha,-\alpha},\psi^\dagger_{\mathbf{k}\beta}\}\rangle=\delta_{\alpha\beta}\omega_g, \tag{A5}$$

$$\langle\{[\psi_{\mathbf{k}\alpha},\hat{H}],\psi^\dagger_{\mathbf{k}\beta}\}\rangle=\delta_{\alpha\beta}(\tau+\tau_u\omega_g)+(\tau-t_{pp})(1-\delta_{\alpha\beta})$$
$$\times(1-\delta_{\alpha,-\beta}) \tag{A6}$$

$$+\delta_{\alpha,-\beta}[\tau+\exp(\imath\mathbf{k}\cdot\mathbf{g}_\alpha)$$
$$\times(\tau_u\omega_g-\tau_u+\tau)], \tag{A7}$$

$$\langle\{[\xi_{\mathbf{k}\alpha,-\alpha},\hat{H}],\psi^\dagger_{\mathbf{k}\beta}\}\rangle$$
$$=\delta_{\alpha\beta}(\tau_u+\tau\omega_g)+(\tau-t_{pp})\omega_g(1-\delta_{\alpha\beta})(1-\delta_{\alpha,-\beta})$$
$$+\delta_{\alpha,-\beta}\{\tau\omega_g+\exp(\imath\mathbf{k}\cdot\mathbf{g}_\alpha)[\tau_u-(\tau_u-\tau)\omega_g]\}, \tag{A8}$$

$$\langle\{[\xi_{\mathbf{k}\alpha,-\alpha},\hat{H}],\xi^\dagger_{\mathbf{k}\beta,-\beta}\}\rangle$$
$$=[\delta_{\alpha\beta}(\tau+\tau_u\omega_g)+(1-\delta_{\alpha\beta})(1-\delta_{\alpha,-\beta})$$
$$\times(\tau-t_{pp})\omega_{\mathbf{g}_\beta+\mathbf{g}_\alpha}]+\delta_{\alpha,-\beta}\{\tau\omega_{2g}+\exp(\imath\mathbf{k}\cdot\mathbf{g}_\alpha)$$
$$\times[\tau_u\omega_g-(\tau_u-\tau)]\}. \tag{A9}$$

[1] Y.Y. Wang, F.C. Zhang, V.P. Dravid, K.K. Ng, M.V. Klein, S.E. Schnatterly, and L.L. Miller, Phys. Rev. Lett. **77**, 1809 (1996).

[2] J. Fink, M. Knupfer, S. Atzkern, and M.S. Golden, J. Electron Spectrosc. Relat. Phenom. **117–118**, 287 (2001).

[3] J.I. Frenkel, Phys. Rev. **37**, 17 (1931).

[4] I. Egri, Phys. Rep. **119**, 364 (1985).

[5] D. Pines, *Elementary Excitations in Solids* (Addison-Wesley, Reading, MA, 1963), Chaps. 3 and 4.

[6] J. Fink, Adv. Electron. Electron Phys. **75**, 121 (1989).

[7] S.E. Schnatterly, Solid State Phys. **34**, 275 (1979).

[8] More precisely one understands excitons as the peaks in $\mathrm{Im}\varepsilon(\mathbf{q},\omega)$. An isolated peak in $\mathrm{Im}\varepsilon(\mathbf{q},\omega)$ corresponds to a shifted peak in $\mathrm{Im}\varepsilon^{-1}(\mathbf{q},\omega)$.

[9] R. Knox, *Theory of Excitons* (Academic Press, New York, 1963).

[10] W. Hanke and L.J. Sham, Phys. Rev. B **21**, 4656 (1980); **12**, 4501 (1975).

[11] S. Albrecht, L. Reining, R. DelSole, and G. Onida, Phys. Rev. Lett. **80**, 4510 (1998); L.X. Benedict, E.L. Shirley, and R.B. Bohn, *ibid.* **80**, 4514 (1998); M. Rohlfing and S.G. Louie, *ibid.* **81**, 2312 (1998).

[12] E.A. Burovski, A.S. Mishchenko, N.V. Prokof'ev, and B.V. Svistunov, Phys. Rev. Lett. **87**, 186402 (2001).

[13] L.J. Sham and T.M. Rice, Phys. Rev. **144**, 708 (1966).

[14] R. Neudert, M. Knupfer, M.S. Golden, J. Fink, W. Stephan, K. Penc, N. Motoyama, H. Eisaki, and S. Uchida, Phys. Rev. Lett. **81**, 657 (1998).

[15] K. Tsutsui, T. Tohyama, and S. Maekawa, Phys. Rev. Lett. **83**, 3705 (1999).

[16] F.H.L. Essler, F. Gebhard, and E. Jeckelmann, Phys. Rev. B **64**, 125119 (2001).

[17] P. Wróbel and R. Eder, Phys. Rev. B **66**, 035111 (2002).

[18] J. Richter, C. Waidacher, and K.W. Becker, Phys. Rev. B **61**, 9871 (2000).

[19] A. Hübsch, J. Richter, C. Waidacher, K.W. Becker, and W. von der Linden, Phys. Rev. B **63**, 205103 (2001).
[20] S. Atzkern, M. Knupfer, M.S. Golden, J. Fink, A. Hübsch, C. Waidacher, K.W. Becker, W. von der Linden, M. Weiden, and C. Geibel, Phys. Rev. B **64**, 075112 (2001).
[21] A. S. Moskvin, J. Málek, M. Knupfer, R. Neudert, J. Fink, R. Hayn, S.-L. Drechsler, N. Motoyama, H. Esaki, and S. Uchida, Phys. Rev. Lett. **91**, 037001 (2003).
[22] F.C. Zhang and K.K. Ng, Phys. Rev. B **58**, 13 520 (1998).
[23] G.H. Wannier, Phys. Rev. **52**, 191 (1937).
[24] P. Fulde, *Electron Correlations in Molecules and Solids* (Springer, Berlin, 1995).
[25] D. Pines and P. Nozieres, *The Theory of Quantum Liquids* (W. A. Benjamin, New York 1966).
[26] V. Ambegaokar and W. Kohn, Phys. Rev. **117**, 423 (1960).
[27] A. A. Abrikosov, L. P. Gorkov, and I. E. Dzyaloshinski, *Methods of Quantum Field Theory in Statistical Physics* (Prentice-Hall, Englewood Cliffs, NJ, 1963).
[28] V. M. Agranovich and V. L. Ginzburg, *Spatial Dispersion in Crystal Optics and The Theory of Excitons*, 2nd ed. (Nauka, Moscow, 1979, Springer-Verlag, Berlin, 1984).
[29] S.-L. Drechsler, J. Málek, and H. Eschrig, Phys. Rev. B **55**, 606 (1997).
[30] R.O. Kuzian, R. Hayn, A.F. Barabanov, and L.A. Maksimov, Phys. Rev. B **58**, 6194 (1998).
[31] A.F. Barabanov and V.M. Beresovskii, Zh. Éksp. Teor. Fiz. **106**, 1156 (1994) [JETP **79**, 627 (1994)].
[32] A.F. Barabanov, R. Hayn, A.A. Kovalev, O.V. Urazaev, and A.M. Belemouk Zh. Éksp. Teor. Fiz. **119**, 777 (2001) [JETP **92**, 677 (2001)].